H_2 purity control of high-pressure alkaline electrolyzers

Martín David [*,**] **Fernando Bianchi** [*]
Carlos Ocampo-Martinez [**] **Ricardo Sánchez-Peña** [*]

[*] *Instituto Tecnológico Buenos Aires (ITBA) and Consejo Nacional de Investigaciones Científicas y Técnicas (CONICET), Ciudad Autónoma de Buenos Aires, Argentina*
[**] *Automatic Control Department, Universitat Politècnica de Catalunya, Institut de Robòtica i Informàtica Industrial (CSIC-UPC), Barcelona, España*

Abstract: This paper proposes a control strategy that mitigates the cross contamination of H_2 and O_2 in a high-pressure alkaline electrolyzer, which consequently increases the supplied gases purity. In order to reduce the diffusion of gases through the membrane, the controller establishes the opening of two outlet valves based on the pressure of the system and the difference in liquid level between both separation chambers. Therefore, a multiple input - multiple output optimal controller is designed here. For this purpose, an available high-fidelity model was simplified in order to obtain a control-oriented model. The proposed controller was evaluated in simulation using the high-fidelity nonlinear model in a wide operating range and was compared with a pair of decoupled PI controllers. The resulting impurity of gases was below 1% in all cases.

Keywords: Hydrogen, alkaline electrolysis, H_2 purity, multivariable control

1. INTRODUCTION

The world economy is constantly expanding along with the demand for energy (IEA, 2019). Furthermore, the extensive use of fossil fuels, with the consequent emission of greenhouse gases, is widely accepted as a situation that needs to change. In this line, global impact studies and environmental protection policies have been formulated (Lux and Pfluger, 2020; Gorre et al., 2019). Around the world, solutions focused on renewable energy sources have been proposed in order to mitigate the emission of greenhouse gases due to the intensive use of fossil fuels. However, the ability to accumulate the excess of energy over long periods of time is needed in order to reach a high integration of renewable energy sources. A widely accepted idea is the use of hydrogen as an energy vector, known as the *hydrogen economy*, which would be an integral solution to produce, store and supply energy (David et al., 2019b; Wang et al., 2019).

Among all the methods of producing sustainable hydrogen, the alkaline electrolysis is presented as the most mature technology. Currently, there is a renewed interest in this technology due to its ease of connection to renewable energy sources (Mahlia et al., 2014). Commonly, the combination of electrolyzers, storage tanks and fuel cells is used as an energy buffer (Dawood et al., 2020). Alkaline electrolysis consists in the splitting of water to form H_2 and O_2 by applying an electric current. The electrolytic cell consists of a pair of electrodes and a membrane made of Zirfon^{TM} that prevent gas mixing. One of the most important challenges of the alkaline electrolysis is the diffusion through this membrane driven by differences in concentration and pressure (Schalenbach et al., 2018). Although the first cause of cross-contamination is inherent in the process and is related to the development of new membranes, the pressure differential can be mitigated by a suitable control design actuating over the outlet valves of both separating chambers.

Despite alkaline electrolysis is a mature technology, its mathematical modelling is still under development. Most models focus only on the cell-stack description but not in the entire system (Haug et al., 2017; Milewski et al., 2014; Hammoudi et al., 2012). Moreover, most of them describe the stationary regime and are built from empirical equations (Amores et al., 2014; Ulleberg, 2003; Hug et al., 1993). Recently, Sánchez et al. (2020) used a commercial software to model the entire system while the cell-stack is described by a semi-empirical approach. In the same direction, some of the authors of the current work have developed a Phenomenological Based Semi-empirical Model (PBSM) reported in David et al. (2019a, 2020). This model has the advantage of describing the dynamic phenomena and the evolution of all the electrolyser subsystems.

Furthermore, to the best of the authors' knowledge, and also from the conclusions reported by Olivier et al. (2017), the design of controllers to solve the problem mentioned above seems to be not addressed yet in the literature. Therefore, the development of useful input-output models for control design is an open research topic (Olivier et al., 2017). In general, control objectives are completely focused on the management of the electrolyzer as an electrical consumer and producer of H_2 connected to a grid (Vivas et al., 2018; Gahleitner, 2013). Moreover, the control of the outlet valves could be found mentioned only by Schug (1998) in his description of a pilot plant. In his work,

an alkaline electrolyzer is described in detail along with experimental results. However, the control system is not detailed enough, but the connection of plant output with control action can be recognized in the simplified flow diagram presented.

Given the lack of control strategies designed for such systems and, in particular, those strategies based on suitable and reliable models properly obtained for control tasks, the main contribution of this paper is twofold. First, from a well-established nonlinear model considering the dynamics and the accurate phenomenology of the alkaline electrolyzers reported in David et al. (2020), a reduced model able to be used as a control-oriented model is obtained and properly validated by using the complete nonlinear model (which, in turn, is validated with real data). Second, by using the reduced model, an optimal controller is designed and the closed-loop performance of the system is evaluated based on the maximization of the hydrogen purity through the mitigation of the cross-contamination of gases into the chambers.

The remainder of the paper is structured as follows. A description of a high-pressure alkaline electrolyzer is presented in Section 2. Next, in Section 3, an optimal model-based controller is designed. Simulation results are presented and discussed in Section 4. Finally, some concluding remarks are gathered in Section 5.

2. HIGH-PRESSURE ALKALINE ELECTROLYZER

As previously mentioned, a proposed solution for energy storage is the combination of an electrolyzer, storage tanks and a fuel cell. In this way, the additional electrical energy is used to produce hydrogen that is stored in the tanks. When renewable energy sources are not able to meet the demand, the stored hydrogen is consumed by the fuel cell.

High-pressure alkaline electrolyzers can supply gases at a storage pressure, dispensing with the use of compressors. However, cross-contamination, i.e., the concentration of O_2 in the H_2 stream and vice versa, increases with pressure, then special attention is required in operation due to safety and quality issues.

Figure 1 shows the piping and instrumentation of a high-pressure alkaline electrolyzer prototype. The components of this system are:

- a pressurized tank (PT) that contains a pack of 15 alkaline electrolytic cells;
- two independent KOH solution circuits with recirculation pumps;
- two gas separation chambers (SC) where the produced gas is split from the liquid KOH solution;
- two heat exchangers for both circuits (HEO and HEH);
- a water injection pump that periodically replenishes the consumed water;
- two outlet lines controlled by two motorized valves (MVO and MVH) connected to storage tanks; and
- an equalization line that connects both bottoms of the SCs.

A detailed description of this system is presented in David et al. (2019a, 2020).

As mentioned in the Introduction, the main objective of an alkaline electrolyzer is to separate water to form H_2 and O_2 by applying an electric current I. In this process, it is highly important to minimize the diffusion through the membrane caused by differences in both concentration and pressure. Up to 2% of H_2 in the O_2 stream is widely accepted as a limit, taking into account that the lower explosive limit of H_2 is 4%. Additionally, H_2 and O_2 gases must be delivered at high pressures in order to avoid the use of compressors. Since gas purity decreases with higher pressures, it is expected to increase the possible operating pressure preventing contamination with a suitable control strategy.

2.1 Control scheme

An alkaline electrolyzer requires several control loops for an efficient and safe operation. The control of both the refrigeration system and the make-up pump ensures a safe operation of the electrolyzer. Whereas, the H_2 production is controlled by the outlet valves. This paper is focused on the latter. A brief description of the other loops is described next.

The refrigeration system and the make-up pump are controlled independently by hysteresis cycles. These control loops, whose designs are not going to be treated in this paper, are defined by the following sets of constraints:

$$\begin{aligned} L_{\mathrm{H_2}} \leq L_{\min} \text{ and } L_{\mathrm{O_2}} \leq L_{\min} &\Rightarrow u_{\mathrm{pump}} = 1, \\ L_{\mathrm{H_2}} \geq L_{\max} \text{ or } L_{\mathrm{O_2}} \geq L_{\max} &\Rightarrow u_{\mathrm{pump}} = 0, \end{aligned} \tag{1}$$

$$\begin{aligned} T_{\mathrm{H_2}} + T_{\mathrm{O_2}} \geq 2\ T_{\max} &\Rightarrow u_{RS} = 1, \\ T_{\mathrm{H_2}} + T_{\mathrm{O_2}} \leq 2\ T_{\min} &\Rightarrow u_{RS} = 0, \end{aligned} \tag{2}$$

where $L_{\mathrm{O_2}}$, $L_{\mathrm{H_2}}$, $T_{\mathrm{O_2}}$ and $T_{\mathrm{H_2}}$ are the liquid solution levels and temperatures in O_2 and H_2 SCs, respectively. These variables are measured by the transmitters LT1, LT2, TT1 and TT2, respectively (see Figure 1). The limits imposed are $L_{\min} = 0.45$ m, $L_{\max} = 0.5$ m, $T_{\min} = 39.5$ °C and $T_{\max} = 40.5$ °C. Finally, the control actions u_{pump} and u_{RS} manage the activation of the injection pump, the refrigeration system pump and the radiator, respectively.

Finally, energy management, with the consequent control of the current-voltage relationship, is intrinsically related to the power sources, so it is beyond the scope of this paper. Details on this topic can be found in Milewski et al. (2014); Sánchez et al. (2020); Speckmann et al. (2019).

As previously indicated, in alkaline electrolysis, a pressure difference between both half-cells generates the gas crossover. Therefore, the control objective is to keep the liquid solution levels equalized in both SCs while H_2 and O_2 are delivered at a certain pressure. This objective is achieved acting over two motorized outlet valves (MVO and MVH in Figure 1). The operating ranges for pressure p and electric current I are 0-7000 kPa and 10-50 A, respectively. It is important to note that this electrolyzer, with an electrode area of $A_{cell} = 143$ cm^2, works in a current density j range between 70-350 mA/cm^2 under the direct relationship

$$j = \frac{I}{A_{cell}}. \tag{3}$$

With the aim of having a suitable resolution in these wide operating ranges and considering the H_2 production

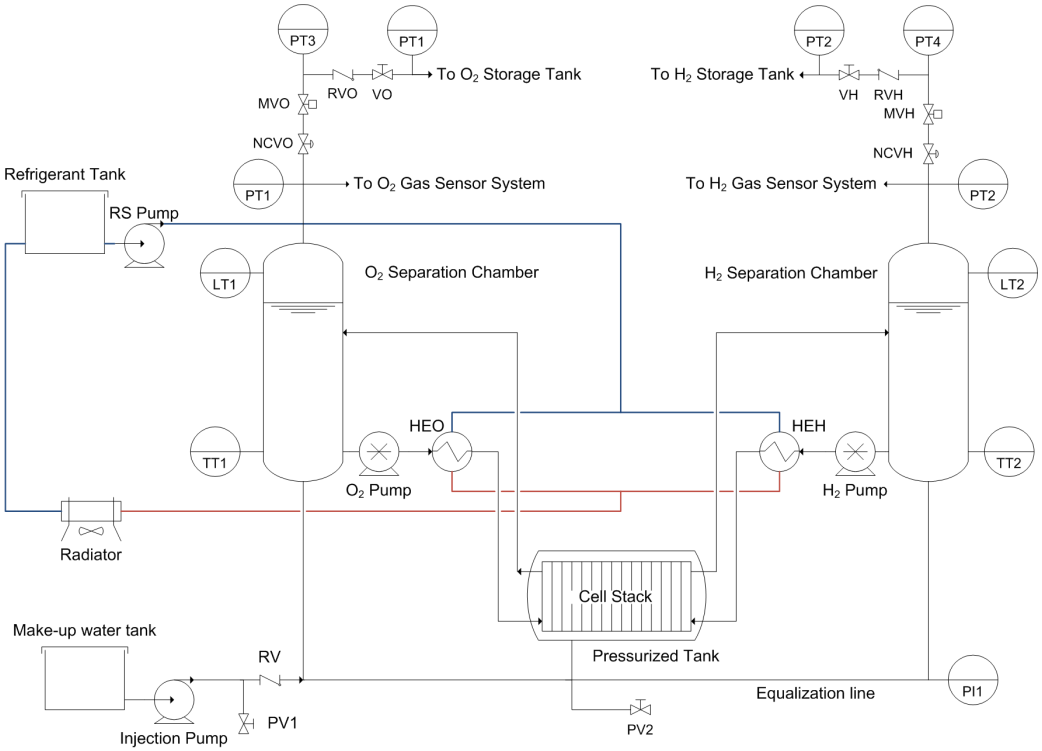

Fig. 1. Piping and instrumentation diagram of the high-pressure alkaline electrolyzer. Taken from David et al. (2020)

capacity of 0.5 Nm^3/h, needle-type outlet valves with a relatively small maximum flow coefficient, e.g., $C_v = 0.004$, must be used. In order to be able to control the system with only one valve per outlet line, the pressure in both storage tanks should be similar.

Another variable to be controlled is the difference between the liquid levels in both SCs, defined as

$$\Delta L = L_{\mathrm{H}_2} - L_{\mathrm{O}_2}. \tag{4}$$

This variable must be kept around a set-point $\Delta L_{\mathrm{ref}} = 0$. This condition will contribute to the natural action of the equalization line circuit by keeping the pressure equalized on both sides of the membrane. In other words, if the control dynamics are slow enough, the equalization line ensures that the pressure in both SCs is almost the same, and the same happens in the electrolytic cells. As stated by Schalenbach et al. (2018), the Zirfon$^{\mathrm{TM}}$ membrane is highly permeable to pressure differences. Finally, controlling the difference in level and pressure generates a high purity of the supplied gases. However, the absence of contamination is unreachable due to the natural diffusion that occurs in the studied process.

The control scheme proposed to achieve the objectives is presented in Figure 2. The controller produces two valve opening values, u_{H_2} and u_{O_2}, taking values between 0 (minimum opening) and 10 (maximum opening). The control values are computed to ensure that

$$P_{\mathrm{H}_2} \to P_{\mathrm{ref}}, \qquad \Delta L \to 0.$$

In normal operation, this pressure is set externally in order to follow smoothly the pressure of the storage tanks P_{tank}. Accordingly, the reference for the pressure P_{ref} is defined as

$$P_{\mathrm{ref}} = P_{\mathrm{tank}} + P_{gap}, \text{ subject to } |dP_{\mathrm{ref}}/dt| < \alpha, \tag{5}$$

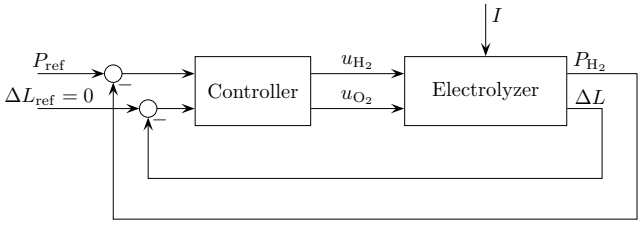

Fig. 2. Proposed control scheme.

being α a rate limit in kPa/s. This rate limit ensures that a sudden change in the storage pressure does not generate an excessive variation in the pressure at both sides of the membrane, with the consequent cross-contamination. Under the assumption of similar pressures, P_{tank} is set equal to P_{H_2}. Moreover, the pressure gap between P_{ref} and P_{tank}, $P_{\mathrm{gap}} = 50$ kPa, is needed to compensate the action of the retention valves (RVO and RVH).

2.2 Reduced control-oriented model

A highly-detailed model for alkaline electrolyzers is given in David et al. (2019a, 2020). This model has 25 differential equations (i.e., 25 states) and 17 additional variables, 50 structural parameters and 49 functional parameters. Such a model is suitable for simulations but not for control design. For this purpose, those variables that produce smaller effects on the controlled variables (ΔL and P_{H_2}) might be neglected under some assumptions and guaranteed conditions that are explained next.

- Although the ultimate goal is to maximize the purity of the gases, the concentrations of impurities are not taken into account for the controller, which is based on the liquid levels and the system pressure.

Table 1. List of states included in the nonlinear reduced model

State	Description
x_1	Molar density in H_2 half-cell
x_2	Concentration of H_2 in H_2 half-cell
x_3	Molar density in O_2 half-cell
x_4	Concentration of O_2 in O_2 half-cell
x_5	Total moles in H_2 SC
x_6	Height of liquid solution level in H_2 SC
x_7	Concentration of H_2 in H_2 SC
x_8	Total moles in O_2 SC
x_9	Height of liquid solution level in O_2 SC
x_{10}	Concentration of O_2 in O_2 SC
x_{11}	Pressure in H_2 SC
x_{12}	Pressure in O_2 SC
x_{13}	Molar flow from the PT to H_2 SC
x_{14}	Molar flow from O_2 SC to the PT

- In addition, despite having two paths of diffusion, i.e., through the membrane and through the equalization line, the latter is smaller than the former. Then, the diffusion through the equalization line can be neglected along with the corresponding states.
- Moreover, under the hypothesis of reaching gas purities greater than 99%, saturation of pure gas in each cell can be assumed in order to calculate diffusion across the membrane.
- Furthermore, according to the ideal gas law, the gas moles behave equally no matter the substance, hence it only matters the accountancy of the number of moles at each line.
- Finally, only the concentrations of pure gases in the electrolytic cells and in the SCs can be considered.

Based on the previous assumptions, the model can be reduced to 14 states, which are listed in Table 1. The rest of the states are considered constant while the parameters, which are represented by algebraic equations, are not modified.

3. CONTROL DESIGN

In this section, a model-based $\mathcal{H}_\infty$ optimal controller is proposed for mitigating the cross-contamination of gases through the membrane in the alkaline electrolyzer presented in Section 2.

A linear model of the electrolyzer is required, therefore the operating conditions of the electrolyzer must be defined. Assuming the control objective of tracking P_{ref} given in (5) and the regulation of ΔL around 0 are satisfied, the operating conditions can be parameterized by the steady-state values of the tank pressure $\bar{P}_{\text{tank}}$ and the current $\bar{I}$. Thus, the system operating region is defined as

$$\mathcal{O} = \left\{ (\bar{P}_{\text{tank}}, \bar{I}) \,:\, 0 \text{ kPa} \leq \bar{P}_{\text{tank}} \leq 7000 \text{ kPa} \right. \\ \left. \text{and } 10 \text{ A} \leq \bar{I} \leq 50 \text{ A} \right\}.$$

Next, the reduced nonlinear model introduced in Section 2.2 is numerically linearized at a representative operating point $(\bar{P}_{\text{tank}}, \bar{I}) \in \mathcal{O}$. To select this point, the linearization is performed over a grid of operating points in $\mathcal{O}$. The magnitude of the frequency responses for these operating points is shown in Figure 3 in gray lines and the selected nominal model is represented by a thicker blue line. This latter model will be used to design the considered linear controllers.

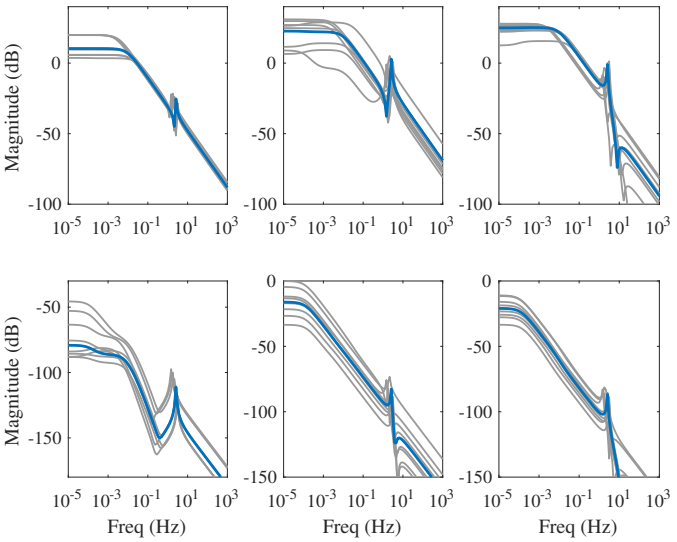

Fig. 3. Frequency responses of the linearized models (gray lines) and the nominal model $G(s)$ (blue lines).

The selected nominal dynamics are approximated by the model

$$y(s) = G(s) \begin{bmatrix} \hat{I}(s) \\ \hat{u}(s) \end{bmatrix} = \begin{bmatrix} G_d(s) & G_c(s) \end{bmatrix} \begin{bmatrix} \hat{I}(s) \\ \hat{u}(s) \end{bmatrix}, \qquad (6)$$

where

$$\hat{u} = \begin{bmatrix} \hat{u}_{\text{H}_2} \\ \hat{u}_{\text{O}_2} \end{bmatrix} = \begin{bmatrix} u_{\text{H}_2} - \bar{u}_{\text{H}_2} \\ u_{\text{O}_2} - \bar{u}_{\text{O}_2} \end{bmatrix}, \qquad y = \begin{bmatrix} P_{\text{H}_2} - \bar{P}_{\text{H}_2} \\ \Delta L \end{bmatrix}.$$

The variable $\hat{u}$ is the vector of control inputs, and y is the vector of the controlled variables. The incremental current $\hat{I} = I - \bar{I}$ acts as a disturbance to be rejected. All of these variables are incremental values with respect to $\bar{I}$, $\bar{u}_{\text{H}_2}$, $\bar{u}_{\text{O}_2}$, and $\bar{P}_{\text{H}_2}$, where the last three variables are functions of the operating point $(\bar{P}_{\text{tank}}, \bar{I})$.

The controller can be designed in the frame of multivariable optimal control. In this case, the control design objectives are expressed as

$$\min_{K(s)} \frac{\|z\|_2}{\|w\|_2}, \qquad (7)$$

where z is a performance variable and w a disturbance. Therefore, the controller design consists in defining a control setup and in selecting z and w according to the control specifications with suitable weighting functions (Sánchez-Peña and Sznaier, 1998).

In the electrolyzer case, tracking a pressure reference P_{ref} while rejecting the disturbance I is sought. Hence, the performance variable z represents the pressure and level errors, and the disturbance w, of the system pressure and the current, i.e.,

$$z = W_e(s) M(s) \begin{bmatrix} P_{\text{H}_2} - P_{\text{ref}} \\ \Delta L \end{bmatrix}, \qquad w = W_u(s) \begin{bmatrix} P_{\text{ref}} \\ \hat{I} \end{bmatrix},$$

where

$$M(s) = \begin{bmatrix} 1 & 0 \\ 0 & 1 \end{bmatrix} \frac{1}{s}, \qquad W_e(s) = \begin{bmatrix} k_{e,1} & 0 \\ 0 & k_{e,2} \end{bmatrix},$$

$$W_u(s) = \begin{bmatrix} k_{u,1} & 0 \\ 0 & k_{u,2} \end{bmatrix} \frac{s/0.1\omega_c + 1}{s/10\omega_c + 1},$$

being $k_{e,j}$, $k_{u,j}$ and ω_c design parameters. The weighting function $M(s)W_e(s)$ penalizes the low frequencies of the

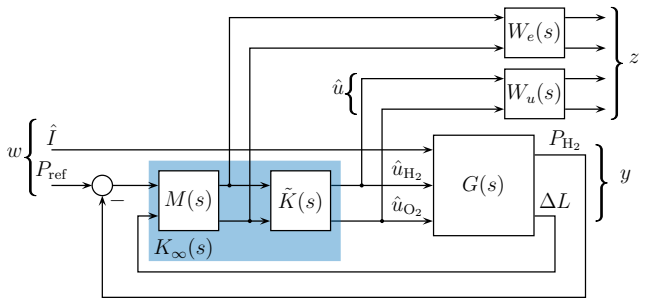

Fig. 4. Control setup for the design of the $\mathcal{H}_\infty$ controller.

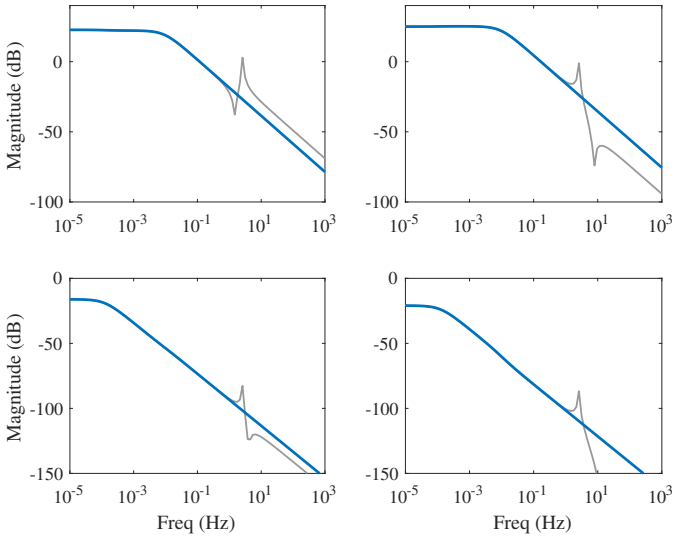

Fig. 5. Frequency responses of the nominal plant (gray) and the reduced plant (blue).

pressure and level errors and $W_u(s)$ penalizes the magnitude at high frequencies of the control actions. The closed-loop setup is shown in Figure 4.

The final controller is obtained after solving the optimization problem (7) and left-multiplying the resulting $\tilde{K}(s)$ by $M(s)$, that is,

$$K_\infty(s) = M(s)\tilde{K}(s). \tag{8}$$

This factorization is needed to ensure the existence of a stabilizing controller.

The order of the controller will be the order of the nominal model plus the order of all the weighting functions. Therefore, to simplify the real-time implementation, the order of $G(s)$ can be numerically reduced. The nominal model of the system to be controlled, namely as $G_c(s)$, exhibits a frequency response similar to a first-order system for each channel. Therefore, using balanced truncation model reduction (Glover, 1984), the plant is approximated by a second order system. The full and reduced models are compared in Figure 5.

4. SIMULATION RESULTS

Numerical simulations were performed with the previously designed controller closing the loop with the full-nonlinear model of the electrolyzer. For comparison purposes, a pair of decoupled PI controllers were also designed. For decoupling the loops, the plant was right-multiplied by the inverse of its DC-gain (Aström and Hägglund, 2006), that is,

$$G_{\text{dec}}(s) = G_c(s)G_c(0)^{-1}.$$

Moreover, the parameters of the PI controllers were:

$$k_{i,1} = 0.18, \quad k_{p,1} = 3, \quad k_{i,2} = 0.16, \quad k_{p,2} = 200.$$

For the $\mathcal{H}_\infty$ controller, the design parameters in the weighting functions were set as

$$k_{e,1} = 0.1, \quad k_{e,2} = 4, \quad k_{u,1} = 0.8, \quad k_{p,1} = 0.8,$$

and $\omega_c = 0.7$ rad/s.

To evaluate the proposed controller, a scenario in which the electrolyzer produces gases at constant pressure but the electric current fluctuates, as if it was provided by renewable energy sources. The resulting simulation using the designed controllers can be seen in Figure 6. As can be noted, both controllers manage to maintain the pressure P_{H_2} close to the reference P_{ref}, with a maximum error of 0.5%, and the level difference in less than 2 mm. Because of this, the O_2 impurity, that is always the highest value, is below 1%. For this particular scenario, the PI controller shows a slightly smaller regulation errors in long term, but the $\mathcal{H}_\infty$ control converges to zero faster that in the PI case after a current change. The performance achieved by both controllers depends on the tuning parameters, the gains in the PI case and the weighting function in the $\mathcal{H}_\infty$ control. The PI controller might be more attractive to practical engineers as it is based on a more intuitive SISO tuning procedure. Nevertheless, this method relies on non-perfect decoupling that can affect the final closed-loop performance. On the other hand, although the $\mathcal{H}_\infty$ controller relies on more sophisticated design tools, it is designed directly and systematically from the MIMO model with less approximations, which could results in a more robust closed-loop system and less design iterations.

5. CONCLUSIONS

In the quest to raise the operating pressure of alkaline electrolyzers, control strategies are needed to decrease gas cross-contamination and, consequently, increase the purity of the supplied gases. In that sense, modelling and control are key issues in operation and design improvements. This work presents a multi-input multi-output optimal controller that was tested in closed loop with a high-fidelity nonlinear model of the electrolyzer. It was able to maintain impurity below 1% in all cases, keeping the liquid solution level difference between both SCs below 4mm and a maximum pressure error of 0.5%.

ACKNOWLEDGEMENTS

This work has been partially funded by the DEOCS project (DPI2016-76493-C3-3R).

REFERENCES

Amores, E., Rodríguez, J., and Carreras, C. (2014). Influence of operation parameters in the modeling of alkaline water electrolyzers for hydrogen production. *International Journal of Hydrogen Energy*, 39, 13063–13078.

Aström, K.J. and Hägglund, T. (2006). *Advanced PID control*. Instrumentation, Systems, and Automation Society, Research Triangle Park, USA.

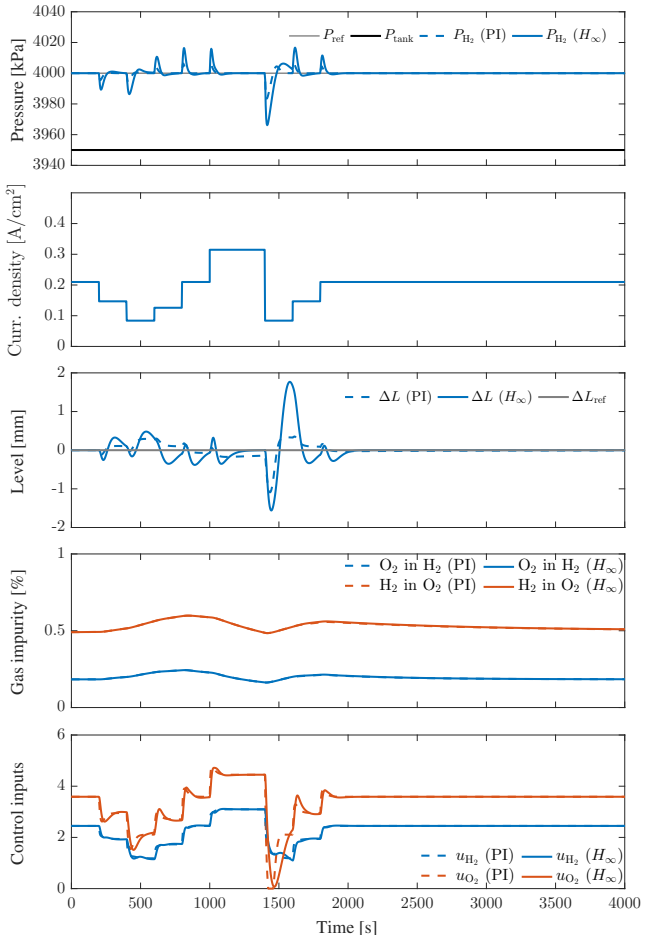

Fig. 6. Closed-loop simulations comparing the responses obtained with the PI controller (dashed lines) and the $\mathcal{H}_\infty$ controller (solid lines).

David, M., Alvarez, H., Ocampo-Martinez, C., and Sánchez-Peña, R. (2019a). Phenomenological based model of hydrogen production using an alkaline self-pressurized electrolyzer. In *18th European Control Conference (ECC)*, 4344–4349.

David, M., Alvarez, H., Ocampo-Martinez, C., and Sánchez-Peña, R. (2020). Dynamic modelling of alkaline self-pressurized electrolyzers: a phenomenological-based semiphysical approach. *International Journal of Hydrogen Energy*, 45, 22394–22407.

David, M., Ocampo-Martinez, C., and Sánchez-Peña, R. (2019b). Advances in alkaline water electrolyzers: A review. *Journal of Energy Storage*, 23, 392–403.

Dawood, F., Anda, M., and Shafiullah, G. (2020). Hydrogen production for energy: An overview. *International Journal of Hydrogen Energy*, 45, 3847–3869.

Gahleitner, G. (2013). Hydrogen from renewable electricity: An international review of power-to-gas pilot plants for stationary applications. *International Journal of Hydrogen Energy*, 38, 2039–2061.

Glover, K. (1984). All optimal Hankel-norm approximations of linear multivariable systems and their L_∞ error bounds. *International Journal of Control*, 39(6), 1115–1193.

Gorre, J., Ortloff, F., and van Leeuwen, C. (2019). Production costs for synthetic methane in 2030 and 2050 of an optimized power-to-gas plant with intermediate hydrogen storage. *Applied Energy*, 253, 114594–114604.

Hammoudi, M., Henao, C., Agbossou, K., Dubé, Y., and Doumbia, M. (2012). New multi-physics approach for modelling and design of alkaline electrolyzers. *International Journal of Hydrogen Energy*, 37, 13895–13913.

Haug, P., Kreitz, B., Koj, M., and Turek, T. (2017). Process modelling of an alkaline water electrolyzer. *International Journal of Hydrogen Energy*, 42, 15689–15707.

Hug, W., Divisek, J., Mergel, J., Seeger, W., and Steeb, H. (1993). Intermittent operation and operation modelling of an alkaline electrolyzer. *International Journal of Hydrogen Energy*, 18(12), 973–977.

International Energy Agency (2019). *Key world energy statistics 2019*. IEA Paris.

Lux, B. and Pfluger, B. (2020). A supply curve of electricity-based hydrogen in a decarbonized european energy system in 2050. *Applied Energy*, 269, 115011–115030.

Mahlia, T., Saktisahdan, T., Jannifar, A., Hasan, M., and Matseelar, H. (2014). A review of available methods and development on energy storage: technology update. *Renewable and Sustainable Energy Reviews*, 33, 532–545.

Milewski, J., Guandalini, G., and Campanari, S. (2014). Modeling an alkaline electrolysis cell through reduced-order and loss-estimate approaches. *Journal of Power Sources*, 269, 203–211.

Olivier, P., Bourasseau, C., and Bouamama, P.B. (2017). Low-temperature electrolysis system modelling: A review. *Renewable and Sustainable Energy Reviews*, 78, 280–300.

Sánchez, M., Amores, E., Abad, D., Rodríguez, L., and Clemente-Jul, C. (2020). Aspen plus model of an alkaline electrolysis system for hydrogen production. *International Journal of Hydrogen Energy*, 45, 3916–3929.

Sánchez-Peña, R. and Sznaier, M. (1998). *Robust System Theory and Applications*. Wiley & Sons.

Schalenbach, M., Zeradjanin, A.R., Kasian, O., Cherevko, S., and Mayrhofer, K.J. (2018). A perspective on low-temperature water electrolysis – challenges in alkaline and acidic technology. *International Journal of Electrochemical Science*, 13, 1173–1226.

Schug, C.A. (1998). Operational characteristics of high-pressure, high-efficiency water-hydrogen-electrolysis. *International Journal of Electrochemical Science*, 23, 1113–1120.

Speckmann, F.W., Bintz, S., and Birke, K.P. (2019). Influence of rectifiers on the energy demand and gas quality of alkaline electrolysis systems in dynamic operation. *Applied Energy*, 250, 855–863.

Ulleberg, O. (2003). Modeling of advanced alkaline electrolyzers: a system simulation approach. *International Journal of Hydrogen Energy*, 28, 21–33.

Vivas, F., De las Heras, A., Segura, F., and Andújar, J. (2018). A review of energy management strategies for renewable hybrid energy systems with hydrogen backup. *Renewable and Sustainable Energy Rev*, 82, 126–155.

Wang, S., Tarroja, B., Smith Schell, L., Shaffe, B., and Scott, S. (2019). Prioritizing among the end uses of excess renewable energy for cost-effective greenhouse gas emission reductions. *Applied Energy*, 235, 284–298.